Int. J. Heat Mass Transfer. Vol. 32, No. 9, pp. 1595–1604, 1989
Printed in Great Britain

0017–9310/89 $3.00 + 0.00
Pergamon Press plc

Heat transfer between a surface and an infiltrated bed of solid particles

V. A. BORODULYA, YU. S. TEPLITSKY, YU. G. YEPANOV and I. I. MARKEVICH

Luikov Heat and Mass Transfer Institute, Minsk, U.S.S.R.

(*Received* 17 *October* 1986)

Abstract—A two-zone model of heat transfer between a surface and an infiltrated disperse bed of solid particles that takes into account the thermal conductivities of wall gas layer and bed particles and the gas-driven convective heat transfer is suggested. Equations obtained on its basis make it possible to describe the laws governing external heat transfer over a wide range of superficial gas velocities (fixed, fluidized and compressed beds). Consideration is given to special cases of heat transfer in developed fluidized and gas-blown fixed beds. The results are presented in the form of simple computational relations. Their validity is checked experimentally and against data available in the literature (including experiments at high temperatures and pressures).

1. INTRODUCTION

HEAT TRANSFER in infiltrated granular beds is of great practical interest, motivated by the problems of chemical technology, drying of dispersed materials, thermal treatment of items in beds of dispersed heat carrier, power engineering and many others. In view of this, a great number of models have been suggested for heat transfer both in fluidized [1–8] and gas-blown fixed beds [9–13]. As a rule, these models are based on assumptions that are limited in character, and therefore the resulting relations are not suited to calculations of heat transfer over a wide range of operating experimental conditions. Thus, for example, heat transfer models and resulting relations for calculating heat transfer coefficients in large particle fluidized beds are suggested in refs. [3, 5–8]. In ref. [12], a model of heat transfer in gas-blown fixed small particle beds was advanced. The foregoing shows that there is a need for further studies with a view to developing universal models that would be based on rather general assumptions about the heat transfer mechanism and that would allow a unified description of its trends in a wide range of gas superficial velocities (fixed, fluidized and compressed beds).

2. PHYSICAL MODEL AND MATHEMATICAL FORMULATION

Heat transfer of a vertical cylinder of radius a and length L is considered. The cylinder is immersed in an infiltrated bed of spherical particles of diameter d.

The proposed model is based on the following assumptions.

(a) The bed is divided into two zones (Fig. 1): a gas interlayer of thickness l_0 which is adjacent to the heat transfer surface and which is a function of the particle diameter and bed voidage, and a quasi-homogeneous medium (a bed of solid particles).

(b) The gas interlayer is characterized by the effective thermal conductivity coefficients λ_f^h, λ_f^v and the bed of solid particles by the coefficients λ_s^h, λ_s^v.

(c) All the heat is carried away from the bed by a filtrating gas.

(d) Local gas velocities in both phases are identical and equal to u/ε.

(e) The thermal and physical properties of the gas are constant.

(f) The difference between the gas and solid particle temperatures in the bed can be neglected.

With consideration for the above assumptions, the mathematical formulation of the heat transfer prob-

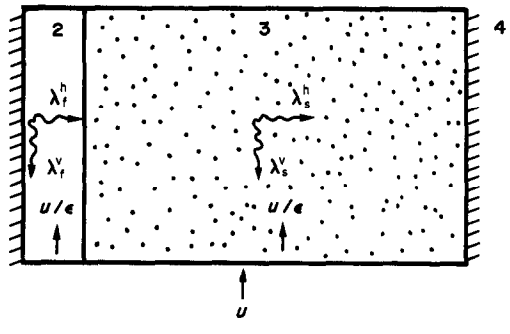

1 Heat transfer surface
2 Gas film
3 Infiltrated disperse bed
4 Apparatus wall

FIG. 1. Heat transfer model.

NOMENCLATURE

a	cylinder radius
Ar	Archimedes number, $d^3 g\rho_f(\rho_s-\rho_f)/\mu_f^2$
c	specific heat
d	diameter of particles
f	dimensionless number, $\sqrt{Pe^*} = \sqrt{(Pe\,\lambda^0/\varepsilon)}$
Fr	Froude number, $(u-u_{mf})^2/gH_{mf}$
g	free fall acceleration
h_w	external heat transfer coefficient
H	bed height
I_0, I_1	first kind modified Bessel function
K_0, K_1	second kind modified Bessel function
K^*	$K_1(s\xi^*)/K_0(s\xi^*)$
l_0	gas film thickness
L	heat transfer surface length
m, n	dimensionless coefficients
Nu	Nusselt number, $h_w d/\lambda_f^c$
Nu^*	Nusselt number, $h_w d/\lambda_f^h$
p	pressure
Pe	Peclet number, $c_f\rho_f u R^2/L\lambda_s^h$
Pr	Prandtl number, $c_f\mu_f/\lambda_f^c$
r, z	coordinates
R	radius of dispersed packing
Re	Reynolds number, $ud\rho_f/\mu_f$
s	$\sqrt{Pe}$
S	surface area of heat transfer probe
T	temperature
T_0	inlet gas temperature
$\langle T\rangle$	average (over two zones) outlet temperature ($z = L$)
u	superficial velocity
w	power of heat transfer probe heater.

Greek symbols

ε	voidage
η	z/L
θ	dimensionless temperature, $(T-T_0)/(T_w-T_0)$
λ	thermal conductivity
λ^0	λ_s^h/λ_f^h
μ	viscosity
ξ	r/R
ξ_a	a/R
ξ_0	l_0/R
ξ^*	$\xi_a+\xi_0$
ρ	density.

Subscripts

f	gas
mf	minimum fluidization
s	solid particles
w	heat transfer surface
∞	fluidized bed core.

Superscripts

c	conductive
h	horizontal
v	vertical
0	at $u = 0$.

lem for a vertical cylinder with constant surface temperature T_w is as follows:

gas film

$$c_f\rho_f\frac{u}{\varepsilon}\frac{\partial T_f}{\partial z} = \lambda_f^v\frac{\partial^2 T_f}{\partial z^2} + \lambda_f^h\left(\frac{\partial^2 T_f}{\partial r^2}+\frac{1}{r}\frac{\partial T_f}{\partial r}\right),$$

$$z>0,\quad a<r<a+l_0; \tag{1}$$

bed of solid particles

$$c_f\rho_f u\frac{\partial T_s}{\partial z} = \lambda_s^v\frac{\partial^2 T_s}{\partial z^2} + \lambda_s^h\left(\frac{\partial^2 T_s}{\partial r^2}+\frac{1}{r}\frac{\partial T_s}{\partial r}\right),$$

$$z>0,\quad a+l_0<r<R; \tag{2}$$

boundary conditions

$$T_f|_{r=a} = T_w;\quad \left.\frac{\partial T_s}{\partial r}\right|_{r=R} = 0;$$

$$T_f = T_s,\qquad \lambda_f^h\frac{\partial T_f}{\partial r} = \lambda_s^h\frac{\partial T_s}{\partial r},$$

$$\text{at } r = a+l_0. \tag{3a}$$

At the boundaries $z = 0$, L, Dankwerts' conditions [14] are used

$$-\lambda_f^v\frac{\partial T_f}{\partial z}+c_f\rho_f\frac{u}{\varepsilon}(T_f-T_0) = 0 \quad \text{at } z = 0$$

$$-\lambda_s^v\frac{\partial T_s}{\partial z}+c_f\rho_f u(T_s-T_0) = 0 \quad \text{at } z = 0$$

$$\frac{\partial T_f}{\partial z} = \frac{\partial T_s}{\partial z} = 0 \quad \text{at } z = L. \tag{3b}$$

3. MATHEMATICAL MODEL

The system of equations (1)–(3b) is rather difficult to analyse and it should therefore be simplified, with the specific features of fluidized and fixed beds being taken into account.

3.1. *Fluidized bed*

Characteristic of developed fluidized beds are high values of thermal conductivity coefficients λ_f^v and λ_s^v, because of intensive mixing of particles throughout the bed space [15]. As a result, the values of the deriva-

tives $\partial T/\partial z$ and $\partial^2 T/\partial z^2$ are small as compared to $\partial T/\partial r$ and $\partial^2 T/\partial r^2$. This fact makes it possible when modelling the fluidized bed heat transfer to ignore completely the dependence of temperatures T_f and T_s on the longitudinal coordinate z and to consider the problem in the one-dimensional approximation. To calculate the terms involving $\partial T/\partial z$ and $\partial^2 T/\partial z^2$ in equations (1) and (2), these derivatives will be replaced by their mean values, which are defined, with the use of condition (3b), as ($L = H$)

$$\left\langle \frac{\partial T_f}{\partial z} \right\rangle = \frac{1}{L}\int_0^L \frac{\partial T_f}{\partial z}\,dz = \frac{1}{L}(T_f|_{z=L} - T_f|_{z=0})$$

$$\left\langle \frac{\partial^2 T_f}{\partial z^2} \right\rangle = \frac{1}{L}\int_0^L \frac{\partial^2 T_f}{\partial z^2}\,dz = \frac{1}{L}\left(\left.\frac{\partial T_f}{\partial z}\right|_{z=L} - \left.\frac{\partial T_f}{\partial z}\right|_{z=0}\right)$$

$$= -\frac{c_f \rho_f u (T_f|_{z=0} - T_0)}{\varepsilon L \lambda_f^v}.$$

Analogously, it will be found that

$$\left\langle \frac{\partial T_s}{\partial z} \right\rangle = \frac{1}{L}(T_s|_{z=L} - T_s|_{z=0})$$

$$\left\langle \frac{\partial^2 T_s}{\partial z^2} \right\rangle = -\frac{c_f \rho_f u (T_s|_{z=0} - T_0)}{L \lambda_s^v}.$$

Replacing $\partial T/\partial z$ and $\partial^2 T/\partial z^2$ in equations (1) and (2) by their mean values gives a one-dimensional approximation

$$\frac{c_f \rho_f u (T_f - T_0)}{\varepsilon L} = \lambda_f^h \left(\frac{d^2 T_f}{dr^2} + \frac{1}{r}\frac{dT_f}{dr}\right),$$

$$a < r < a + l_0 \qquad (4)$$

$$\frac{c_f \rho_f u (T_s - T_0)}{L} = \lambda_s^h \left(\frac{d^2 T_s}{dr^2} + \frac{1}{r}\frac{dT_s}{dr}\right),$$

$$a + l_0 < r < R. \qquad (5)$$

The system of equations (4) and (5), subject to condition (3a), simulates heat transfer of a vertical cylinder in a developed fluidized bed.

3.2. *Gas-blown fixed bed*

The convective motion of particles being absent, the thermal conductivity coefficients λ_f^v and λ_s^v are by several orders of magnitude smaller than in a bubbling bed. Here, therefore, variations of temperatures T_f and T_s along the coordinate z should not be neglected, and the problem of heat transfer in a fixed bed should be considered in a two-dimensional form. Since the Peclet numbers $c_f \rho_f u L/\varepsilon \lambda_f^v$, $c_f \rho_f u L/\lambda_s^v \gg 1$ (the estimates λ_f^v and λ_s^v are taken to be λ_f^e and $0.1 c_f \rho_f u d$ [12]), it is permissible to disregard longitudinal heat conduction in equations (1) and (2) as compared to convective heat transfer in both zones. Equations (1) and (2) then reduce to the form

$$c_f \rho_f \frac{u}{\varepsilon}\frac{\partial T_f}{\partial z} = \lambda_f^h \left(\frac{\partial^2 T_f}{\partial r^2} + \frac{1}{r}\frac{\partial T_f}{\partial r}\right),$$

$$z > 0, \quad a < r < a + l_0 \qquad (6)$$

$$c_f \rho_f u \frac{\partial T_s}{\partial z} = \lambda_s^h \left(\frac{\partial^2 T_s}{\partial r^2} + \frac{1}{r}\frac{\partial T_s}{\partial r}\right),$$

$$z > 0, \quad a + l_0 < r < R. \qquad (7a)$$

Boundary conditions for $z = 0$ follow from equation (3b)

$$T_f = T_s = T_0 \qquad (7b)$$

when longitudinal heat conduction is ignored.

Equations (6) and (7a), subject to conditions (3a) and (7b), model heat transfer of a vertical cylinder in a gas-blown fixed bed.

In the limiting case of

$$Pe = \frac{c_f \rho_f u R^2}{L \lambda_s^h} \gg 1, \quad Pe^* = \frac{c_f \rho_f u R^2}{\varepsilon L \lambda_f^h} \gg 1$$

the gradients $\partial T/\partial z \ll \partial T/\partial r$ and it is again permissible, as for a fluidized bed, to disregard temperature variations along the coordinate z in both zones. Replacing the partial derivatives $\partial T_f/\partial z$ and $\partial T_s/\partial z$ in equations (6) and (7a) by their mean values—obtained with the use of condition (7b)—again gives a system of equations (4) and (5). Thus, with conditions (3a), these equations describe heat transfer in both a developed fluidized bed and a gas-blown fixed bed (when Pe, $Pe^* \gg 1$).

It must only be borne in mind that in a fluidized bed the quantity L in equations (4) and (5) should be substituted by the bed height H.

4. ANALYSIS OF THE MODEL

4.1. *Fluidized bed*

The heat transfer coefficient is defined as

$$h_w = \frac{\lambda_f^h}{T_s(R) - T_w}\left.\frac{dT_f}{dr}\right|_{r=a}. \qquad (8)$$

The solution of equations (4) and (5), subject to conditions (3a), can be easily obtained analytically. This allowed the following expression to be derived for the coefficient h_w:

$$h_w = \frac{\lambda_f^h}{R} f s \xi^* \frac{I_1(f\xi_a)c_1 - K_1(f\xi_a)c_2}{1 - s\xi^* c} \qquad (9)$$

where

$$\xi^* = \xi_a + \xi_0; \quad c_1 = \lambda^0 s\gamma + f\gamma_0; \quad c_2 = \lambda^0 s\beta + f\beta_0;$$

$$c = \lambda^0 s[I_0(f\xi_a)\gamma + K_0(f\xi_a)\beta] + f[I_0(f\xi_a)\gamma_0 + K_0(f\xi_a)\beta_0];$$

$$\gamma = -I_1(s)K_1(s\xi^*)K_0(f\xi^*) + K_1(s)I_1(s\xi^*)K_0(f\xi^*);$$

$$\gamma_0 = I_1(s)K_0(s\xi^*)K_1(f\xi^*) + K_1(s)I_0(s\xi^*)K_1(f\xi^*);$$

$$\beta = I_1(s)K_1(s\xi^*)I_0(f\xi^*) - K_1(s)I_1(s\xi^*)I_0(f\xi^*);$$

$$\beta_0 = I_1(s)K_0(s\xi^*)I_1(f\xi^*) + K_1(s)I_0(s\xi^*)I_1(f\xi^*).$$

Since the solid phase in a developed fluidized bed is stirred rather vigorously (horizontal thermal conductivity of a fluidized bed λ_s^h is high [16]), of that the values of the parameter $\lambda^0 = \lambda_s^h/\lambda_f^h$ are high ($\lambda^0 \sim 10^4$–10^5) and Pe are relatively small ($Pe \sim 10^{-2}$–10^0), equation (9) can be significantly simplified. The estimates have demonstrated that for $l_0/a \ll 1$, equation (9) may yield an extremely simple relation with an error not exceeding 6%

$$h_w \cong \frac{\lambda_f^h}{l_0}. \tag{10}$$

Equation (10) has a simple physical meaning: owing to a high thermal conductivity of a developed fluidized bed λ_s^h, the magnitude of its heat transfer coefficient is determined only by the gas film resistance. Just as in ref. [5], the thermal conductivity coefficient λ_f^h of the gas film will be represented as the sum of the conductive and convective (filtrational) components: $\lambda_f^h = \lambda_f^c + nc_f\rho_f(u/\varepsilon)d$. The gas film thickness l_0 is a function of the mean free path length of gas and is defined as [3]

$$l_0 = md(1-\varepsilon)^{-2/3}.$$

With inclusion of expressions for λ_f^h and l_0, equation (10) will transform into

$$h_w = \frac{\lambda_f^c(1-\varepsilon)^{2/3}}{md} + \frac{n}{m}\frac{c_f\rho_f u(1-\varepsilon)^{2/3}}{\varepsilon} \tag{11}$$

where the dimensionless quantities m and n are the empirical coefficients of the model considered, and are to be found from comparison with experimental data.

4.2. *Gas-blown fixed bed (great Pe and Pe*)*

Here, too, equation (9) is valid, because, as pointed out above, heat transfer in a fixed bed at high Pe and Pe^* is modelled by a system of equations (4) and (5) with conditions (3a). This case is characterized by small values of $\lambda^0 = \lambda_s^h/\lambda_f^h$ ($\lambda^0 \sim 10^0$–10^1) as compared with a fluidized bed. Note that in a gas-blown fixed bed the value of λ_s^h is determined from [17]

$$\lambda_s^h = \lambda_s^0 + Bc_f\rho_f ud \tag{12}$$

where λ_s^0 is the value of λ_s^h for $u = 0$ and $0.07 < B < 0.15$ (depending on the shape of particles). When $Pe \gg 1$ and $l_0/a \ll 1$, equation (9) can also be significantly simplified to

$$h_w = \frac{\lambda_f^h}{R}\frac{\lambda^0 sK^* + f^2\xi_0}{1+\lambda^0 sK^*\xi_0} \tag{13a}$$

where $K^* = K_1(s\xi^*)/K_0(s\xi^*)$. This equation shows that heat transfer in a ventilated fixed bed is determined by the thermal resistance of both the gas film and the disperse bed itself. Moreover, the rate of heat transfer of a cylindrical probe depends on its diameter. Note that for a plane heat transfer surface $K^* = 1$. In this case, equation (13a) takes the form

$$h_w = \frac{\lambda_f^h}{R}\frac{\lambda^0 s + f^2\xi_0}{1+\lambda^0 s\xi_0}. \tag{13b}$$

4.3. *Gas-blown fixed bed (arbitrary Pe and Pe*)*

For convenience of analysis, the system of equations (6) and (7a), subject to conditions (3a) and (7b), is stated in dimensionless form as follows:

$$Pe\frac{\lambda^0}{\varepsilon}\frac{\partial\theta_f}{\partial\eta} = \frac{\partial^2\theta_f}{\partial\xi^2} + \frac{1}{\xi}\frac{\partial\theta_f}{\partial\xi}, \quad \eta > 0, \quad \xi_a < \xi < \xi_a + \xi_0 \tag{14}$$

$$Pe\frac{\partial\theta_s}{\partial\eta} = \frac{\partial^2\theta_s}{\partial\xi^2} + \frac{1}{\xi}\frac{\partial\theta_s}{\partial\xi}, \quad \eta > 0, \quad \xi_a + \xi_0 < \xi < 1 \tag{15}$$

$$\theta_f|_{\xi=\xi_a} = 1; \quad \theta_f|_{\eta=0} = \theta_s|_{\eta=0} = 0; \quad \left.\frac{\partial\theta_s}{\partial\xi}\right|_{\xi=1} = 0;$$

$$\theta_f = \theta_s, \quad \frac{\partial\theta_f}{\partial\xi} = \lambda^0\frac{\partial\theta_s}{\partial\xi}, \quad \text{at } \xi = \xi_a + \xi_0. \tag{16}$$

It is seen that the dimensionless temperatures θ in both zones are functions of the following parameters: Pe, λ^0, ε, ξ_a, and ξ_0. According to results obtained in ref. [3], it was assumed in calculations involving equations (14)–(16) that $l_0 = 0.1d$. The bed voidage was taken to be equal to 0.4. The system of equations (14)–(16) was solved numerically by the time-dependent technique with the use of a stable implicit finite-difference scheme [18]. Owing to the smallness of ξ_0, non-uniform spacings are chosen in ξ.

Over the segment $\xi \in [\xi_a, \xi_a + \xi_0]$, the spatial step h_1 is taken to be equal to $h\xi_0$, where h is the step over the segment $\xi \in [\xi_a + \xi_0, 1]$. A grid with a uniform step h was selected in the η-direction. In order to elucidate the dependence of the accuracy of numerical solutions, on the magnitude of h, preliminary calculations were carried out on different grids for several typical versions. It was found that to achieve an accuracy of 2–5% for the heat transfer coefficients over the range $0.01 \leqslant Pe \leqslant 10\,000$, it is sufficient that h be taken equal to 0.02.

The numerical solution allowed the determination of the temperature fields in both zones and of the heat transfer coefficients:

mean heat transfer coefficients

$$\langle Nu_c^*\rangle = \frac{\langle q\rangle d}{\lambda_f^h}\Bigg/\frac{\langle T\rangle - T_0}{\ln\dfrac{T_w - T_0}{T_w - \langle T\rangle}};$$

$$\langle Nu_1^*\rangle = \frac{\langle q\rangle d}{\lambda_f^h}\Big/(T_w - T_0);$$

$$\langle Nu_2^*\rangle = \frac{\langle q\rangle d}{\lambda_f^h}\Big/(T_w - \langle T_s(z,R)\rangle); \tag{17}$$

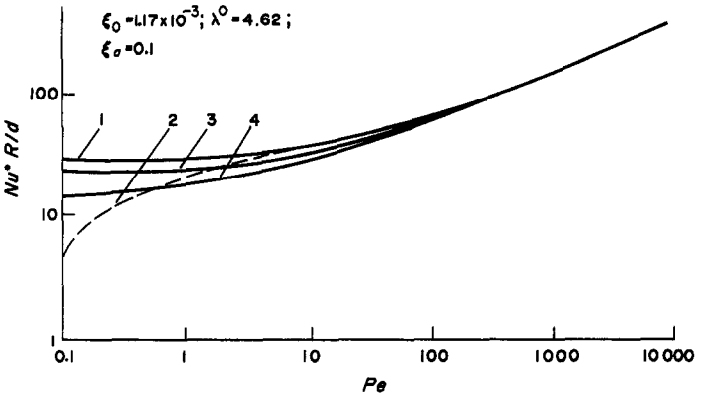

FIG. 2. Dimensionless heat transfer coefficients vs Pe ($T_w = 100°C$, $T_0 = 20°C$): 1, 2, $\langle Nu_2^* \rangle$ and $\langle Nu_c^* \rangle$ according to the two-dimensional model of equations (14)–(16) at $\xi_a = 0.1$; 3, 4, Nu^* according to equations (9) and (13a).

local heat transfer coefficients

$$Nu_3^* = \frac{qd}{\lambda_f^h} \Big/ (T_w - T_0);$$

$$Nu_4^* = \frac{qd}{\lambda_f^h} \Big/ [T_w - T_s(z, R)]. \qquad (18)$$

The heat flux q was determined from

$$q = -\frac{\lambda_f^h (T_w - T_0)}{R} \frac{\partial \theta_f}{\partial \xi}\Big|_{\xi = \xi_a}. \qquad (19)$$

The integration of formula (19) gave the average values $\langle q \rangle$; the mean temperatures $\langle T \rangle$ and $\langle T_s(z, R) \rangle$ were found analogously.

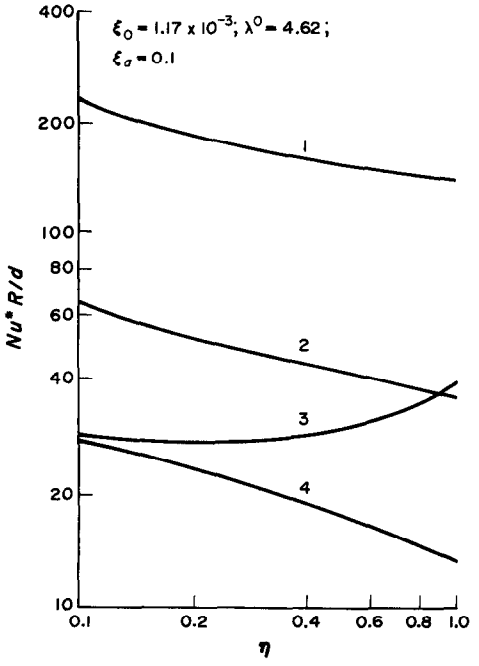

FIG. 3. Local dimensionless heat transfer coefficients vs dimensionless longitudinal coordinate: 1, Nu_3^*, Nu_4^* ($Pe = 3158$); 2, Nu_3^*, Nu_4^* ($Pe = 31.58$); 3, 4, Nu_4^*, Nu_3^* ($Pe = 1.05$).

The predicted mean and local heat transfer coefficients and the cross-section mean temperature $\eta = \text{const}$. are presented in Figs. 2–4. It was found that for $Pe > 10$ the heat transfer coefficients predicted by different equations were essentially the same, whereas there was an appreciable difference between them at small values of Pe. Figure 2 also contains the curves plotted by equations (9) and (13a) that describe heat transfer in the one-dimensional approximation. It can be seen that with $Pe > 100$ the heat transfer coefficients predicted by the two-dimensional model, by equations (14)–(16) and by one-dimensional equations (9) and (13a) virtually coincide. As shown by the analysis, the case of large values of Pe ($Pe > 100$) comprises rather a wide class of practically important systems with fixed ventilated beds of solid particles. The analysis of heat transfer data for such systems can be carried out on the basis of relation (13a).

5. EXPERIMENTAL SETUP

External heat transfer of a disperse bed was investigated experimentally in a cylindrical column, with

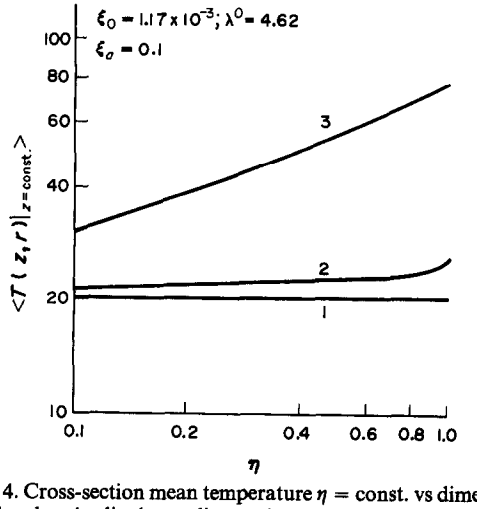

FIG. 4. Cross-section mean temperature $\eta = \text{const}$. vs dimensionless longitudinal coordinate: 1, $Pe = 3158$; 2, 31.58; 3, 1.05 ($T_w = 100°C$, $T_0 = 20°C$).

Table 1. Characteristics of disperse materials

Disperse material	d (mm)	u_{mf} (m s^{-1})	ε_{mf}	ρ_s (kg m^{-3})
Glass beads	1.75	0.85	0.40	2650
Chamotte	3.0	0.95	0.48	2300
Peas	5.7	1.35	0.42	1400
Millet	2.0	0.55	0.39	1000

an i.d. of 300 mm, equipped with a perforated gas distributor. The heat transfer probe used was a copper cylinder, 30 mm o.d. and 150 mm long, with a wall thickness of 5 mm and an electrical heater placed inside. The height of the disperse material bed varied from 510 to 710 mm. The probe was positioned vertically along the column axis 200 mm above the distributor. The characteristics of disperse materials are listed in Table 1. All the experiments were carried out at room temperature and atmospheric pressure. The fluidizing agent was air. Temperature measurements were made by chromel–coppel thermocouples with 0.2 mm diameter wire. The coefficient of heat transfer between the infiltrated bed of solid particles and the probe surface was determined with a maximum error of 5% by the steady-state technique [18] with the aid of the following formula :

$$h_w = \frac{W}{S[T_w - T_s(R)]}. \quad (20)$$

6. EXPERIMENTAL RESULTS AND THEIR CORRELATION

6.1. *Developed fluidized bed*

The results obtained are presented in Figs. 5 and 6 as plots of the coefficient h_w vs the air filtration velocity. The data on heat transfer in a fluidized bed were correlated with the aid of equation (11). The values of the coefficients m and n were found to be: $m = 0.14$, $n = 0.0061$. As a result, the following semi-empirical correlation was obtained for calculating the coefficient of heat transfer in a developed fluidized bed:

$$h_w = \frac{7.2\lambda_f^c}{d}(1-\varepsilon)^{2/3} + 0.044 c_f \rho_f u \frac{(1-\varepsilon)^{2.3}}{\varepsilon} \quad (21)$$

or in dimensionless form

$$Nu = 7.2(1-\varepsilon)^{2/3} + 0.044 Pr\, Re \frac{(1-\varepsilon)^{2/3}}{\varepsilon}. \quad (22)$$

Comparison of the experimental data and those available in the literature with the results predicted by equations (21) and (22) is illustrated in Figs. 6 and 7. The standard deviation of experimental points from those predicted by equation (22) is 18% (Fig. 7). It is important to note that equation (22) also reproduces well the data obtained for high-temperature fluidized beds [20, 21, 24]. The mean bed voidage was determined from the following relations:

large particles ($d > 1$ mm) [3]

$$\varepsilon = \varepsilon_{mf} + 1.56 \frac{Re - Re_{mf}}{Ar^{1/2}}(1-\varepsilon_{mf}); \quad (23)$$

small particles ($d < 1$ mm) [25]

$$\varepsilon = 1 - \frac{1-\varepsilon_{mf}}{1 + 0.7(H_{mf}/2R)^{1/2} Fr^{1/3}}. \quad (24)$$

In these equations the dominating temperature was taken to be the temperature of the bed $T_\infty = T_s(R)$. In calculations of the heat transfer coefficients, the dominating temperature was taken to be the temperature $[T_s(R) + T_w]/2$ as recommended in ref. [26].

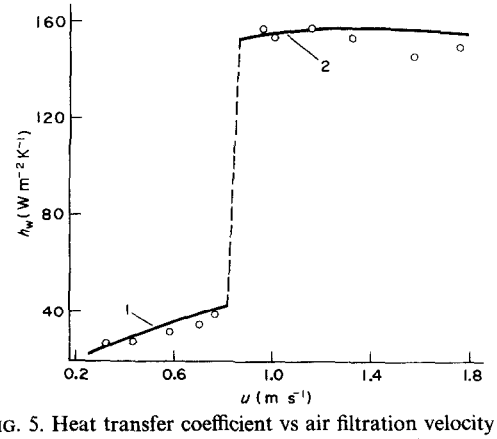

FIG. 5. Heat transfer coefficient vs air filtration velocity: 1, calculation by equation (13a); 2, calculation by equation (21). Glass beads.

6.2. *Gas-blown fixed bed*

The data obtained are shown in Figs. 5 and 8. Correlation was made with the aid of analytical relation (13a)—applicable, as shown above, when $Pe > 100$. The thermal conductivity of the gas-blown disperse packing and the gas film thickness in equation (13a) were determined from

$$\lambda_s^h = \lambda_s^0 + 0.1 c_f \rho_f u d, \quad l_0 = 0.1d. \quad (25)$$

The thermal conductivity of the gas film was given by

$$\lambda_f^h = \lambda_f^c + 0.0061 c_f \rho_f u d/\varepsilon \quad (26)$$

where the factor 0.0061 is selected on the basis of the experiments in a fluidized bed.

It is seen from Fig. 8 that equation (13a) satisfactorily reproduces the data obtained in the present work. The figure also contains the h_w values calculated from Gabor's equation [12]:

$$h_w = \sqrt{\left(\frac{4 c_f \rho_f u \lambda_s^h}{\pi L}\right)} + \frac{\lambda_s^h}{2a}. \quad (27)$$

Equation (27) overestimates the results by 20–30%. This can be attributed to the fact that this equation is based on the heat transfer model which disregards the

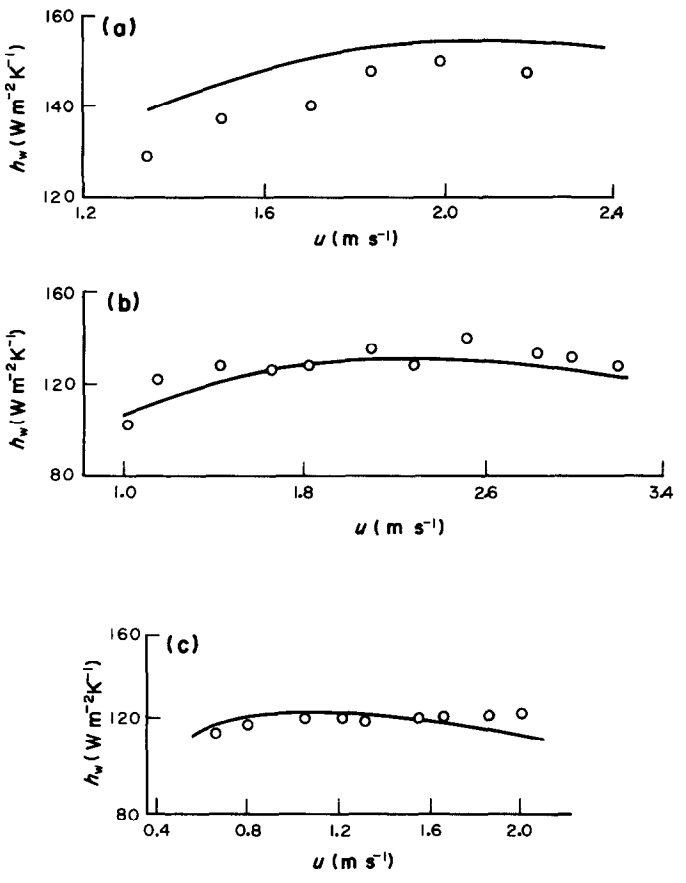

FIG. 6. Comparison between measured and predicted values of the heat transfer coefficient for a fluidized bed. ○, experimental data; ——, prediction by equation (21): (a) peas; (b) chamotte; (c) millet.

presence of a gas film near the heat transfer surface and assumes a constant bulk voidage of the bed [12].

Figure 9 compares the h_w values predicted by equation (13a) with the experimental data of ref. [13] obtained at different pressures of permeating gas. Some discrepancy is observed only for beds of copper spheres (Fig. 9(c)), but the agreement becomes better when the probe height in equation (13a) is replaced by the bed height.

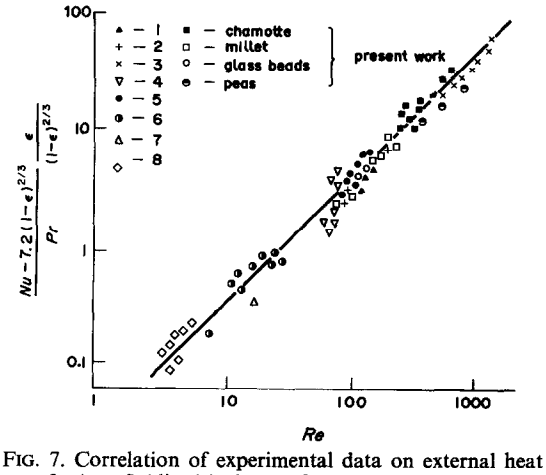

FIG. 7. Correlation of experimental data on external heat transfer in a fluidized bed: 1, ref. [6] (d = 1.58 mm, T_∞ = 293 K); 2, ref. [7] (d = 1.3 mm, T_∞ = 293 K); 3, ref. [7] (d = 4.0 mm, T_∞ = 293 K); 4, ref. [20] (d = 1.17 mm, T_∞ = 1073 K); 5, ref. [21] (d = 1.8 mm, T_∞ = 1123 K); 6, ref. [22] (d = 0.26 mm, T_∞ = 293 K); 7, ref. [23] (d = 0.70 mm, T_∞ = 293 K); 8, ref. [24] (d = 0.29 mm, T_∞ = 773 K).

Figure 10 gives a comparison between the predicted and experimental results [3] on heat transfer rate in a compressed packed bed of glass beads. It is seen from the figure that the h_w values predicted by equation (13a) agree rather well (the maximum deviation is 13%) with those measured for $Re \geqslant 1200$. As Re decreases, these deviations increase and attain 45%. This can be attributed to some specific features of the experiment—namely to the fact that the thermocouple which measured the bed temperature was located at a small distance from the probe. This naturally overestimated the h_w values. The overestimation was especially appreciable at small filtration velocities (small values of Re).

We now analyse the effect of a gas interlayer on the coefficient h_w. When $l_0 = 0$, equation (13a) transforms into

$$h_w = \frac{\lambda_s^h}{R} sK^* = \sqrt{\left(\frac{c_f \rho_f u \lambda_s^h}{L}\right)} K^*. \qquad (28)$$

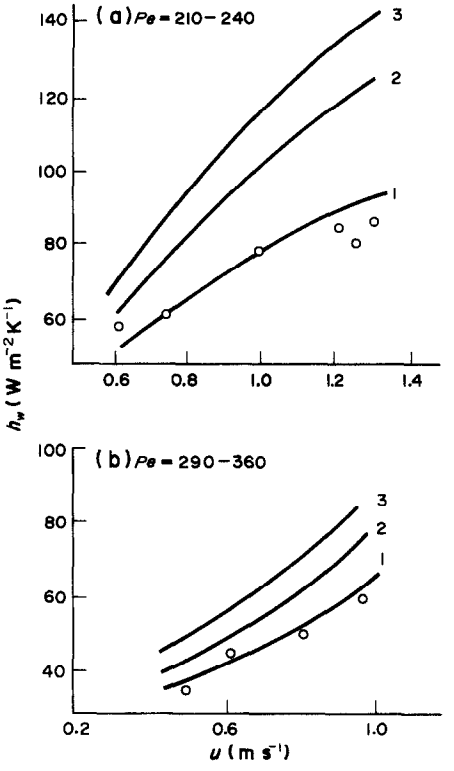

FIG. 8. The heat transfer coefficient of a gas-blown fixed bed vs air filtration velocity. ○, experimental data; 1, prediction by equation (13a); 2, prediction by equation (28); 3, prediction by equation (27): (a) peas; (b) chamotte.

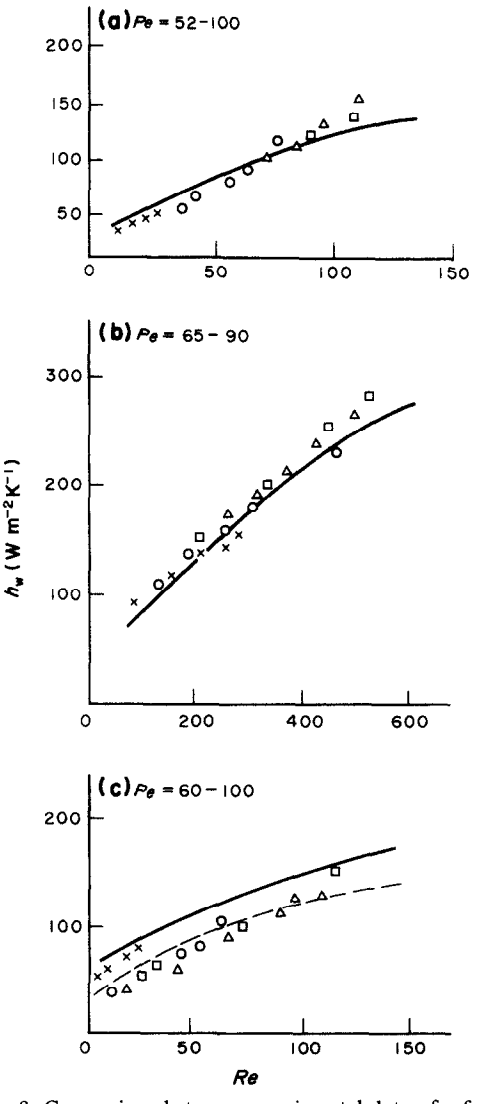

FIG. 9. Comparison between experimental data of ref. [13] and those predicted by the two-zone model. ×, $p = 0.1$ MN m^{-2}; ○, 0.38; △, 0.65; □, 0.93: (a) sand, $d = 1.02$ mm, air; (b) sand, $d = 2.37$ mm, air; (c) copper, $d = 0.62$ mm, air. Dashed line in Fig. 9(c) is prediction by equation (13a), L is the granular bed height ($H_{mf} = 380$ mm).

The h_w values predicted by equation (28) are shown in Fig. 8. Naturally, they agree better with the calculations using Gabor's equation (27), which also disregards the thermal resistance produced by the high-porosity zone (gas film) at the heat transfer surface. The data of ref. [12] and the estimates made in the present work show that the thermal resistance of a gas film in a bed of fine particles ($d < 0.8$ mm) can be ignored, and relations (27) and (28) can be used. Presumably, this can be explained by a smaller effective thickness of the gas film for finer particles and its smaller contribution to the overall thermal resistance.

7. CONCLUSIONS

A two-zone model of external heat transfer in infiltrated disperse systems has been developed. The involvement of a gas film at the heat transfer surface and of the effect of granular bed thermal conductivity (λ_s) on heat transfer renders the problem rather universal, thus making it possible to describe the trends of external heat transfer within a wide range of gas filtration velocities (fixed, fluidized and compressed beds).

Analytical equation (9) describes the dependence of the heat transfer coefficient on governing factors in both developed fluidized and gas-blown fixed beds (when $Pe > 100$). It can be reduced to equations (10) and (13a), depending on the λ_s^h values typical of fluidized and gas-blown fixed beds. It is these latter equations on which the correlation of the available experimental data on heat transfer in infiltrated disperse beds is based.

Semi-empirical relation (21), obtained in this paper, describes the present and literature data on the quantity h_w in fluidized beds within a wide range of experimental conditions (including high temperature experiments).

Equation (13a), for which the values of λ_s^h, l_0, and λ_f^h are determined from equations (25) and (26), makes it possible to describe experimental values of h_w in

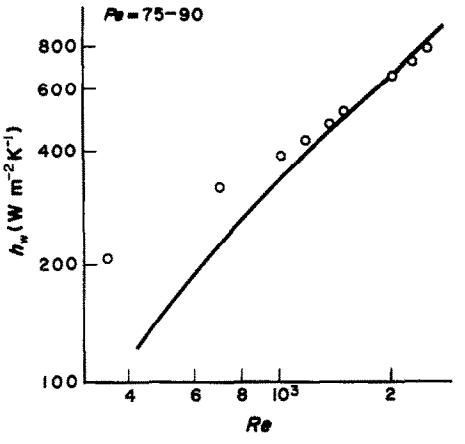

FIG. 10. Comparison between experimental data of ref. [3] and those predicted by equation (13a). Glass beads, $d = 3.1$ mm (fixed compressed bed).

gas-blown fixed beds at both normal and elevated pressures of a filtrating gas.

REFERENCES

1. A. P. Baskakov, B. V. Berg, A. F. Ryzhkov and I. F. Filippovsky, *Heat and Mass Transfer Processes in a Fluidized Bed.* Izd. Metallurgiya, Moscow (1978).
2. N. V. Antonishin, M. A. Geller and V. I. Ivanyutenko, Heat transfer in a pseudo-turbulent disperse bed with allowance for the filtrational component, *J. Engng Phys.* **43,** 360–364 (1982).
3. V. A. Borodulya, V. L. Ganzha and V. I. Kovenskiy, *Hydrodynamics and Heat Transfer in a Pressurized Fluidized Bed.* Izd. Nauka i Tekhnika, Minsk (1982).
4. V. L. Ganzha, S. N. Upadhyay and S. S. Saxena, A mechanistic theory for heat transfer between fluidized beds of large particles and immersed surfaces, *Int. J. Heat Mass Transfer* **25,** 1531–1540 (1982).
5. S. S. Zabrodsky, Yu. G. Epanov, D. M. Galershtein, S. C. Saxena and A. K. Holar, Heat transfer in a large-particle fluidized bed with immersed in-line and staggered bundles of horizontal smooth tubes, *Int. J. Heat Mass Transfer* **24,** 571–579 (1981).
6. F. W. Staub, Solids circulation in turbulent fluidized beds and heat transfer to immersed tube banks, *J. Heat Transfer* **101,** 391–396 (1979).
7. N. M. Catipovic, Heat transfer to horizontal tubes in fludized beds: experiment and theory, Ph.D. Thesis, Oregon State University (1979).
8. N. Decker and L. R. Glicksman, Heat transfer in large particles fluidized beds, *Int. J. Heat Mass Transfer* **26,** 1307–1320 (1983).
9. M. E. Aerov, O. M. Todes and D. A. Narinsky, *Stationary Granular-bed Apparatus.* Izd. Khimiya, Leningrad fluidization, *Chem. Engng Sci.* **25,** 979–984 (1970).
10. V. A. Mukhin and I. I. Smirnova, Investigation of heat and mass transfer processes in filtration through porous media, Preprint 26–27 of the Institute of Thermal Physics, Novosibirsk (1978).
11. Yu. A. Buyevich and Ye. B. Perminov, Unsteady-state heating of a fixed granular bed, *J. Engng Phys.* **38,** 29–37 (1980).
12. J. D. Gabor, Heat transfer to particle beds with gas flows less than or equal to that required for incipient fluidization, *Chem. Engng Sci.* **25,** 979–984 (1970).
13. J. S. M. Botterill and A. O. O. Denloye, A theoretical model of heat transfer to a packed or quiescent fluidized bed, *Chem. Engng Sci.* **33,** 509–515 (1978).
14. P. V. Dankwerts, Continuous flow systems. Distribution of resistance times, *Chem. Engng Sci.* **2,** 1–10 (1953).
15. O. E. Potter, Mixing. In *Fluidization* (Edited by J. F. Davidson and D. Harrison), pp. 293–382. Academic Press, London (1971).
16. V. A. Borodulya, Yu. G. Yepanov and Yu. S. Teplitsky, Horizontal mixing of particles in a free fluidized bed, *J. Engng Phys.* **42,** 767–773 (1982).
17. N. I. Gelperin and V. G. Ainstein, Heat transfer in fluidized beds. In *Fluidization* (Edited by J. F. Davidson and D. Harrison), pp. 454–495. Academic Press, London (1971).
18. A. A. Samarsky and Ye. S. Nikolayev, *Solution Methods for Network Equations.* Izd. Nauka, Moscow (1978).
19. V. A. Osipova, *Experimental Investigation of Heat Transfer Processes.* Izd. Energiya, Moscow (1979).
20. A. I. Tamarin, Yu. G. Yepanov, N. S. Rassudov and V. N. Shemyakin, Investigation of heat transfer in a fluidized-bed furnace to a horizontal staggered bundle, *Energomashinostroyeniye* No. 12, 7–8 (1977).
21. A. V. Ryzhakov, V. I. Babiy, Yu. G. Pavlov, V. N. Sukhova, S. S. Novoselov, S. P. Titov and G. F. Nikitina, Analysis of the products of Irsha-Borodino brown coal combustion in a bench fluidized bed combustor, *Teploenergetika* No. 11, 31–35 (1980).
22. N. I. Gelperin, V. G. Ainstein and A. V. Zaikovsky, Concerning the mechanism of heat transfer between a surface and non-uniform granular material bed, *Khim. Prom.* No. 6, 18–26 (1966).
23. B. Nenkirchen and H. Blenke, Gestaltung horizontaler Rohrbündel in Gas-Wirbelschichtreaktoren nach wärmetechnischen Gesichtspunkten, *Chemie-Ingr-Tech.* **45,** 307–312 (1972).
24. A. T. Tishchenko and Yu. I. Khvostukhin, *Fluidized-bed Furnaces and Heat Exchangers.* Izd. Naukova Dumka, Kiev (1973).
25. A. I. Tamarin and Yu. S. Teplitsky, Investigation of non-uniform fluidized bed expansion, *J. Engng Phys.* **32,** 469–473 (1977).
26. S. S. Zabrodsky, N. V. Antonishin, G. M. Vasiliyev and A. L. Parnas, Selection of a computational relation for determining the coefficient of heat transfer between a high-temperature fluidized bed and a body immersed in it, *Izv. Akad. Nauk BSSR, Ser. FEN* No. 4, 103–107 (1974).

TRANSFERT DE CHALEUR ENTRE UNE SURFACE ET UN LIT INFILTRE DE PARTICULES SOLIDES

Résumé—Un modèle à deux zones du transfert de chaleur entre une surface et un lit infiltré de particules solides dispersées est suggéré pour prendre en compte les conductivités thermiques de la couche de gaz à la paroi et des particules du lit, ainsi que le transfert thermique convectif par le gaz. Des équations obtenues permettent la description des lois qui gouvernent le transfert thermique externe pour un large domaïne de vitesses du gaz superficiel (lits fixes, fluidisés et comprimés). Les résultats sont présentés sous forme de relations simples pour le calcul. Leur validité est testée expérimentalement et à l'aide de données disponibles dans la littérature (en incluant des expériences à température et pression élevées).

WÄRMEÜBERGANG ZWISCHEN EINER OBERFLÄCHE UND EINER DURCHSTRÖMTEN SCHICHT FESTER PARTIKEL

Zusammenfassung—Es wird ein Zwei-Zonen-Modell des Wärmeübergangs zwischen einer durchströmten Schicht fester Partikel vorgeschlagen, das die Wärmeleitfähigkeit der gasförmigen Wandschicht und der Partikel sowie den konvektiven Wärmetransport berücksichtigt. Die ermittelten Gleichungen ermöglichen die Beschreibung des äußeren Wärmeübergangs in einem weiten Bereich der überlagerten Gasgeschwindigkeiten (feste, fluidisierte und verdichtete Schichten). Spezialfälle der Wärmeübertragung in fluidisierten und in festen gasdurchströmten Schichten werden berücksichtigt. Die Ergebnisse sind in Form einfacher mathematischer Beziehungen dargestellt. Ihre Gültigkeit wird experimentell und mit Daten aus der Literatur überprüft (einschließlich Experimenten bei hohen Temperaturen und Drücken).

ТЕПЛООБМЕН МЕЖДУ ПОВЕРХНОСТЬЮ И СЛОЕМ ТВЕРДЫХ ЧАСТИЦ, ПРОДУВАЕМЫМ ГАЗОМ

Аннотация—Предложена двухзонная модель теплообмена между поверхностью и продуваемым дисперсным слоем твердых частиц, учитывающая теплопроводность пристенной прослойки газа, слоя частиц и конвективный перенос тепла газом. Полученные на её основе уравнения позволяют описывать закономерности внешнего теплообмена в широком диапазоне скоростей фильтрации газа (неподвижный, кипящий и зажатый слои). Как частные случаи рассмотрен теплообмен в развитом кипящем и инфильтруемом неподвижном слоях. Результаты представлены в виде простых расчетных соотношений. Их справедливость проверена экспериментально и путем сопоставления с литературными данными (включая опыты при высоких температурах и повышенных давлениях).